blood® Regular Article

LYMPHOID NEOPLASIA

Targeted sequencing in DLBCL, molecular subtypes, and outcomes: a Haematological Malignancy Research Network report

Stuart E. Lacy,[1,*] Sharon L. Barrans,[2,*] Philip A. Beer,[3,*] Daniel Painter,[1] Alexandra G. Smith,[1] Eve Roman,[1] Susanna L. Cooke,[4] Camilo Ruiz,[3] Paul Glover,[2] Suzan J. L. Van Hoppe,[2] Nichola Webster,[2] Peter J. Campbell,[3] Reuben M. Tooze,[5] Russell Patmore,[6] Cathy Burton,[2,†] Simon Crouch,[1,†] and Daniel J. Hodson[7,†]

[1]Epidemiology and Cancer Statistics Group, Department of Health Sciences, University of York, York, United Kingdom; [2]Haematological Malignancy Diagnostic Service, St. James's Institute of Oncology, Leeds, United Kingdom; [3]Wellcome Trust Sanger Institute, Hinxton, Cambridge, United Kingdom; [4]Institute of Cancer Sciences, University of Glasgow, Glasgow, United Kingdom; [5]Section of Experimental Haematology, Leeds Institute of Molecular Medicine, University of Leeds, Leeds, United Kingdom; [6]Queen's Centre for Oncology and Haematology, Castle Hill Hospital, Cottingham, United Kingdom; and [7]Wellcome–MRC Cambridge Stem Cell Institute, University of Cambridge, Cambridge, United Kingdom

KEY POINTS

- **Robust subtypes of DLBCL are identified by model-based clustering of genetic mutations in a large (n = 928) population-based cohort.**
- **With full follow-up data available for all sequenced patients, the prognostic significance of these subtypes is identified.**

Based on the profile of genetic alterations occurring in tumor samples from selected diffuse large B-cell lymphoma (DLBCL) patients, 2 recent whole-exome sequencing studies proposed partially overlapping classification systems. Using clustering techniques applied to targeted sequencing data derived from a large unselected population-based patient cohort with full clinical follow-up (n = 928), we investigated whether molecular subtypes can be robustly identified using methods potentially applicable in routine clinical practice. DNA extracted from DLBCL tumors diagnosed in patients residing in a catchment population of ∼4 million (14 centers) were sequenced with a targeted 293-gene hematological-malignancy panel. Bernoulli mixture-model clustering was applied and the resulting subtypes analyzed in relation to their clinical characteristics and outcomes. Five molecular subtypes were resolved, termed MYD88, BCL2, SOCS1/SGK1, TET2/SGK1, and NOTCH2, along with an unclassified group. The subtypes characterized by genetic alterations of BCL2, NOTCH2, and MYD88 recapitulated recent studies showing good, intermediate, and poor prognosis, respectively. The SOCS1/SGK1 subtype showed biological overlap with primary mediastinal B-cell lymphoma and conferred excellent prognosis. Although not identified as a distinct cluster, NOTCH1 mutation was associated with poor prognosis. The impact of TP53 mutation varied with genomic subtypes, conferring no effect in the NOTCH2 subtype and poor prognosis in the MYD88 subtype. Our findings confirm the existence of molecular subtypes of DLBCL, providing evidence that genomic tests have prognostic significance in non-selected DLBCL patients. The identification of both good and poor risk subtypes in patients treated with R-CHOP (rituximab, cyclophosphamide, doxorubicin, vincristine, and prednisone) clearly show the clinical value of the approach, confirming the need for a consensus classification. (*Blood*. 2020;135(20):1759-1771)

Introduction

Diffuse large B-cell lymphoma (DLBCL) is the most common non-Hodgkin lymphoma.[1-3] Although potentially curable with immunochemotherapy, refractory or relapsed lymphoma occurs in ∼40% of patients. Despite the substantial increase in biological understanding in recent years, attempts to improve survival by combining standard therapy with novel targeted agents have thus far yielded disappointing results, with no phase 3 trial leading to a change in the accepted standard of care since the addition of rituximab to cyclophosphamide, doxorubicin, vincristine, and prednisone (R-CHOP) chemotherapy in 2002.[4] One barrier to the effective use of novel therapies targeting specific pathways is the biological heterogeneity of DLBCL and the likely existence of multiple distinct disease subtypes. Hence, to permit more accurate targeting in clinical trials, it is becoming increasingly important to define these subtypes, permitting stratification that separates patients likely to achieve cure with R-CHOP alone from high-risk groups that may benefit from emerging therapies.

Gene expression profiling distinguishes transcriptional subtypes of DLBCL, including activated B-cell–like (ABC) and germinal center B-cell–like (GCB) in the cell-of-origin classification, and more recently, molecular high-grade (MHG).[5-8] Genomic studies have reported additional heterogeneity[9-15]; the 3 latest used whole-exome sequencing to describe molecular subtypes based on the profile of genetic alterations within each tumor.[16-18] Two of these studies proposed partially overlapping classifications[16,17]; these converging conclusions suggest the existence of convincing molecular subtypes with distinct biology and the potential to guide therapeutic targeting.

However, several questions remain before a consensus classification can be implemented in clinical practice. The first relates to robustness, because it is unclear how variation introduced by different sequencing platforms, variant calling algorithms, biopsy material, and methods of statistical analysis affect the ability to resolve genetic subtypes. The second relates to the practicalities of implementing a classification in a real-world setting: the ability to resolve genetic subtypes using panel-based sequencing on DNA from both fresh and formalin-fixed, paraffin-embedded (FFPE) material. Finally, studies conducted to date have been largely based on specimens and data from clinical trials and specialist referral center archives, potentially limiting the generalizability of findings to the patient population as a whole.

Established with the aim of addressing such questions, the current report describes results from a genomics study embedded within a contemporary UK "real-world" population-based patient cohort. All diagnoses in the catchment population of ~4 million (14 hospitals) are centrally made at a specialized hematological oncology reference laboratory.[19] Using surplus material archived at the time of diagnosis, 4244 lymphoid and myeloid tumor samples have now been sequenced and assessed for somatic mutations against a pan-hematological malignancy panel of 293 genes; the findings for 928 patients diagnosed with DLBCL are reported here.

Materials and methods

Patients and procedures

Data are from the UK population-based Haematological Malignancy Research Network (HMRN; https://www.hmrn.org).[19] Initiated in 2004, all diagnoses within HMRN's boundaries are made and coded by clinical specialists at a single integrated hematopathology laboratory, the Haematological Malignancy Diagnostic Service (www.HMDS.info). Full details of HMRN's methods and ethical approvals have been published elsewhere; ethical approval for HMRN was granted under REC reference 04/Q1205/69 and for the genetic sequencing under 14/WS/0098.[19,20] In brief, covering 14 hospitals and tracking all patients with hematological malignancies (~2400 per year) through clinical and national administrative systems (mortality and morbidity), HMRN's patient cohort operates under a legal basis that permits full treatment and outcome data to be collected from clinical records without explicit consent. The study cohort for the current report comprised 2358 subjects newly diagnosed with DLBCL between 1 September 2004 and 31 August 2012 with International Classification of Diseases for Oncology, Third Edition, codes 9679, 9680, 9688, 9712, and 9735. Of these patients, 928 (39.4%) had suitable diagnostic material for genetic analysis (supplemental Figure 1, available on the *Blood* Web site). All patients were followed up for mortality until 31 December 2018.

DNA sequencing

DNA was extracted from surplus FFPE material archived at the time of diagnostic biopsy using the Qiagen QIAamp DNA FFPE tissue kit (catalog no. 51306). For each sample, 50 to 200 ng of genomic DNA was sheared by using a Covaris LE220 focused ultrasonicator (Covaris) to produce 100 to 200 bp fragments. Indexed libraries were generated by using a modified version of the SureSelect XT protocol (Agilent Technologies), pooled (16-plex), and captured with a bespoke set of 120 nt biotinylated RNA baits (Agilent Technologies); this approach covered 293 genes implicated in hematological malignancy (supplemental Table 1) using the SureDesign interface (Agilent Technologies) on default parameters (all coding exons of all genes targeted with 10 flanking bases at 3′ and 5′ end of each exon). Capture libraries were quantified, assessed for size distribution and quality, and sequenced on Illumina HiSeq 2500 instruments using 75 base paired-end sequencing according to the manufacturer's instructions. The average read depth across all samples was 500× reads per base. Full details of sequencing, variant calling, and annotation are provided in the supplemental Methods (section 2.1). Single nucleotide variants and copy number variants are detailed in supplemental Tables 2 and 3.

Statistical analysis

A total of 117 genetic features occurred in at least 1% of patients; these features defined binary variables denoting 105 mutations, 4 amplifications, and 8 markers indicating presence of either a homozygous deletion or mutation (supplemental Table 1). These 117 binary variables were used to identify subgroups of patients with similar genetic characteristics. Genetic features found in $<1\%$ of cases were not used for clustering.

To identify these genetic subgroups, the data were modeled as a finite mixture of Bernoulli distributions, providing a data-driven probabilistic interpretation of group membership strength.[21] The number of identifiable clusters was selected by using the Akaike Information Criterion (AIC) likelihood penalization method.

Three additional techniques were used to assess cluster strength and stability. First, the Integrated Completed Likelihood (ICL)[22] was used to determine cluster number; second, cluster stability under repeated resampling was investigated by consensus clustering[23]; and third, the clustering process was restricted to the homogeneous group of de novo DLBCL not otherwise specified (NOS) patients treated with R-CHOP ($n = 579$). Full details of this sensitivity analysis are presented in the supplemental Methods (sections 2.2-2.4).

Survival analysis was conducted by using the Kaplan-Meier estimator and proportional hazards regression, with all patients followed up for mortality until 31 December 2018. Analyses were conducted in Stata 15.1[24] and R 3.5.3,[25] using the libraries flexmix[21] and survival.[26] Gene expression profiling was available for a subset of cases from a previous analysis, in which full details of the methods are provided.[7,8] Gene Set Enrichment Analysis was run using software developed by the Broad Institute.[27,28] Pearson's χ^2 test was used for assessing differences in proportions, with the Benjamini-Hochberg adjustment for multiple comparisons. The data used in this study are presented in supplemental Tables 4 and 6; the R-code is available on Github, at: https://github.com/ecsg-uoy/DLBCLGenomicSubtyping.

Results

Genetic substructure of DLBCL

Demographic and clinical characteristics of the study cohort (N = 2358) and analysis cohort (n = 928) are summarized in Table 1. Although broadly similar to the study cohort as a whole, those with archived material of sufficient quality for next-generation sequencing (analysis cohort) were, on average, slightly younger (median diagnostic age 68.5 vs 70.0 years), were more likely to have localized disease (eg, 33% vs 30.5% stage I/II disease), and were more likely to have been treated with curative intent (86.5% vs 81.8%).

Individual biopsy samples were associated with a median of 7 driver mutations (supplemental Figure 2). In 49 patients (5.3%), no genetic abnormality was detected. Genetic alterations stratified according to cell of origin confirmed that when applied to FFPE material, our sequencing platform and variant calling strategy identified mutational profiles in close agreement with previous studies (supplemental Figure 2).[16-18]

Applying the Akaike Information Criterion to determine optimal cluster number, 5 genomic clusters were identified. These were named MYD88, BCL2, TET2/SGK1, SOCS1/SGK1, and NOTCH2, according to the genetic features most enriched in each cluster, leaving 27% of patients as "not elsewhere classified" (NEC) (Figure 1). Information on the genetic clusters identified using the integrated completed likelihood criterion and an assessment of cluster stability by consensus clustering are presented in the supplemental Methods (sections 2.2 and 2.3; supplemental Figures 3-7; supplemental Table 5).

The MYD88 cluster (n = 152) was dominated by mutation of *MYD88* (L265P), *PIM1*, *CD79B*, and *ETV6* and frequent loss of *CDKN2A*; the available gene expression data showed that most belonged to the ABC subtype, with enrichment for signatures associated with ABC-DLBCL, IRF4, and MYC (Figure 2). To assess biological features of DLBCL independent of anatomic site of presentation, we included special site DLBCL in our primary clustering. However, very similar results were observed when such cases were excluded and clustering restricted to DLBCL NOS (supplemental Figure 8). The majority of primary central nervous system lymphomas (PCNSL), along with primary testicular and those with breast involvement, clustered within this group (Table 2). This cluster strongly recapitulates the recently described MCD[16] and C5[17] subtypes.

The BCL2 cluster (n = 176) showed frequent mutation of *EZH2*, *BCL2*, *CREBBP*, *TNFRSF14*, *KMT2D*, and *MEF2B*. The majority of cases for whom fluorescence in situ hybridization (FISH) was available (82 of 92) had a t(14:18) BCL2 translocation, and mutation of *BCL2* was strongly correlated with this translocation ($P < .0001$). Gene expression revealed a predominance of GCB-DLBCL but also enrichment for MHG DLBCL (Table 2; Figure 2). Most cases of transformed follicular lymphoma fell within this cluster, robustly mapping to the previously described EZB and C3 clusters.[16,17]

The SOCS1/SGK1 group (n = 111) was characterized by mutations, including *SOCS1*, *CD83*, *SGK1*, *NFKBIA*, *HIST1H1E*, and *STAT3*. Several of these genes, including SOCS1, were known targets of aberrant somatic hypermutation. This cluster seems to represent a subdivision of the recently described C4 cluster.[17]

SOCS1 mutation is a finding shared with primary mediastinal B-cell lymphoma (PMBCL). The inclusion of cases diagnosed as PMBCL in our clustering allowed the demonstration that 12 of 20 PMCBL cases clustered in this group along with 98 DLBCL NOS cases. The latter cases in this cluster showed no pathological features of PMBCL and were not enriched for mediastinal involvement (supplemental Figure 9). Gene expression profiling showed that DLBCL NOS cases in this group were predominantly of GCB origin and enriched for signatures associated with PMBCL and JAK/STAT signaling, suggesting a degree of biological similarity to PMBCL[29] (Figure 2). Enrichment was also seen for other genes previously noted to be enriched in PMBCL, including ITPKB, NFKBIE, and CIITA.[30] These results suggest that PMBCL, a lymphoma with a unique anatomic location, shares significant molecular overlap with a subset of otherwise nodal DLBCL, supporting a previous description of non-mediastinal DLBCL tumors that share biological similarity to PMBCL.[29] This also recapitulates the findings observed for the relation between PCNSL, primary testicular and primary breast DLCBL, and the MYD88 group of DLCBL NOS, supporting a more general overlap between special site lymphomas and specific molecular subsets of DLBCL NOS.

The TET2/SGK1 (n = 98) cluster was characterized by mutations including *TET2*, *SGK1*, *KLHL6*, *ZFP36L1*, *BRAF*, *MAP2K1*, and *KRAS*. The mutation of multiple components of the ERK pathway was associated with enrichment of gene expression signatures of RAS and ERK (Figure 2). Predominantly GCB in origin, these cases seem to represent a second subdivision of the recently described C4 cluster.[17]

A final NOTCH2 cluster (n = 143) was characterized by mutations including *NOTCH2*, *BCL10*, *TNFAIP3*, *CCND3*, *SPEN*, *TMEM30A FAS*, and *CD70*. Our targeted panel did not capture *BCL6* fusion status, although *BCL6* rearrangement by using FISH, where available (317 of 928), confirmed a strong correlation with *NOTCH2* mutation ($P < .0001$). Gene expression showed that this cluster comprised a mixture of ABC, GCB, and unclassified DLBCL (Table 2). Enhanced NOTCH activity was not detected by gene expression, nor could we detect transcriptional evidence of increased NOTCH activity when restricting analysis to patients with *NOTCH2* mutation. The mutational similarities suggest biological similarity to marginal zone lymphoma; a preexisting diagnosis of marginal zone lymphoma was noted only in 3 patients. This group corresponds closely to the previously described BN2[16] or C1[17] subtypes.

Validation of our clustering strategy on an external data set

To further explore the relation of clusters defined in our data sets to those of other cohorts recently defined, we took advantage of published data from Chapuy et al.[17] We considered this from 2 angles: first, by applying our Bernoulli clustering approach to their total data set; and second, by restricting analysis to the features in common between our data set and theirs. With respect to the former, our algorithm identified 6 clusters, largely recapitulating those published by Chapuy et al (supplemental Figure 10). Genetic features enriched within these clusters closely matched those enriched in the data of Chapuy et al, as

Table 1. Patient and tumor characteristics: DLBCL newly diagnosed within HMRN, September 2004 to August 2012

Characteristic	Study cohort	Analysis cohort			
			DLBCL NOS		
		Total	All patients	R-CHOP treated	De novo R-CHOP treated
All subtypes combined	2358 (100)	928 (100)	839 (100)	609 (100)	579
DLBCL NOS	2170 (92.0)	839 (90.4)	–	–	–
PCNSL	74 (3.1)	33 (3.6)	–	–	–
Primary mediastinal	54 (2.3)	20 (2.2)	–	–	–
T-cell/histiocyte-rich	31 (1.3)	21 (2.3)	–	–	–
Plasmablastic	24 (1.0)	14 (1.5)	–	–	–
Intravascular	5 (0.2)	1 (0.1)	–	–	–
Age at diagnosis (range), y	70.0 (1.6-97.8)	68.5 (8.5-97.8)	68.8 (8.5-97.8)	66.3 (22.8-89.0)	66.1 (22.8-89.0)
Male sex, n (%)	1231 (52.2)	500 (53.9)	451 (53.8)	326 (53.5)	309 (53.4)
Performance status (ECOG)					
0-1	1423 (60.3)	588 (63.4)	540 (64.4)	448 (73.6)	448 (77.4)
≥2	680 (28.8)	256 (27.6)	219 (26.1)	120 (19.7)	120 (20.7)
Not known*	255 (10.8)	84 (9.1)	80 (9.5)	41 (6.7)	11 (1.9)
Stage (Ann Arbor)					
I	337 (14.3)	145 (15.6)	137 (16.3)	111 (18.2)	111 (19.2)
II	383 (16.2)	161 (17.3)	149 (17.8)	139 (22.8)	139 (24.0)
III	313 (13.3)	157 (16.9)	148 (17.6)	124 (20.4)	124 (21.4)
IV	900 (38.2)	321 (34.6)	269 (32.1)	184 (30.2)	184 (31.8)
Not fully staged/not known*	425 (18.0)	144 (15.5)	136 (16.2)	51 (8.4)	21 (3.6)
IPI					
Low	445 (20.3)	213 (23.0)	192 (22.9)	178 (29.2)	178 (30.8)
Low/intermediate	365 (16.7)	143 (15.4)	128 (15.3)	110 (18.1)	110 (19.0)
Intermediate/high	394 (18.0)	156 (16.8)	146 (17.4)	116 (19.0)	116 (20.1)
High	462 (19.6)	167 (18.0)	150 (17.9)	95 (15.6)	95 (16.4)
Not known*	692 (29.3)	249 (26.8)	223 (26.6)	110 (18.1)	80 (13.8)
Cell of origin					
Classic†					
GCB	410 (49.7)	265 (50.5)	252 (52.7)	181 (52.6)	172 (53.6)
ABC	233 (28.2)	142 (27.0)	141 (29.5)	99 (28.8)	91 (28.3)
Unclassified	182 (22.1)	118 (22.5)	85 (17.8)	64 (18.6)	58 (18.1)
Refined†					
GCB	359 (43.5)	234 (44.6)	223 (46.7)	163 (47.4)	155 (48.3)
ABC	228 (27.6)	140 (26.7)	139 (29.1)	98 (28.5)	90 (28.0)
MHG	60 (7.3)	34 (6.5)	32 (6.7)	20 (5.8)	19 (5.9)
Unclassified	178 (21.6)	117 (22.3)	84 (17.6)	63 (18.3)	57 (17.8)
Treated curatively	1929 (81.8)	803 (86.5)	730 (87.0)	609 (100.0)	579 (100.0)
R-CHOP treated	1536 (65.1)	648 (69.8)	609 (72.6)		
Median survival (95% CI), y	4.1 (3.4-4.9)	6.2 (5.5-7.2)	6.4 (5.6-7.5)	10.2 (8.3-11.9)	10.6 (8.4-12.5)
R-CHOP treated (95% CI), y	9.3 (8.3-10.6)	10.4 (8.4-12.5)	10.2 (8.3-11.9)		
5-y OS (95% CI),%	47.7 (45.7-49.7)	54.6 (51.5-57.9)	55.4 (52.1-58.8)	67.3 (63.6-71.1)	68.0 (64.3-71.9)
R-CHOP treated (95% CI), %	62.8 (60.4-65.2)	67.5 (64.0-71.2)	67.3 (63.6-71.1)		

Data are presented as n (%) unless otherwise indicated. CI, confidence interval; ECOG, Eastern Cooperative Oncology Group; IPI, International Prognostic Index; OS, overall survival.

*Includes transformed follicular lymphoma (study cohort, n = 169; analysis cohort, n = 55) where baseline information is taken at the time of first diagnosis but not at transformation.

†Percentage of those with material available.

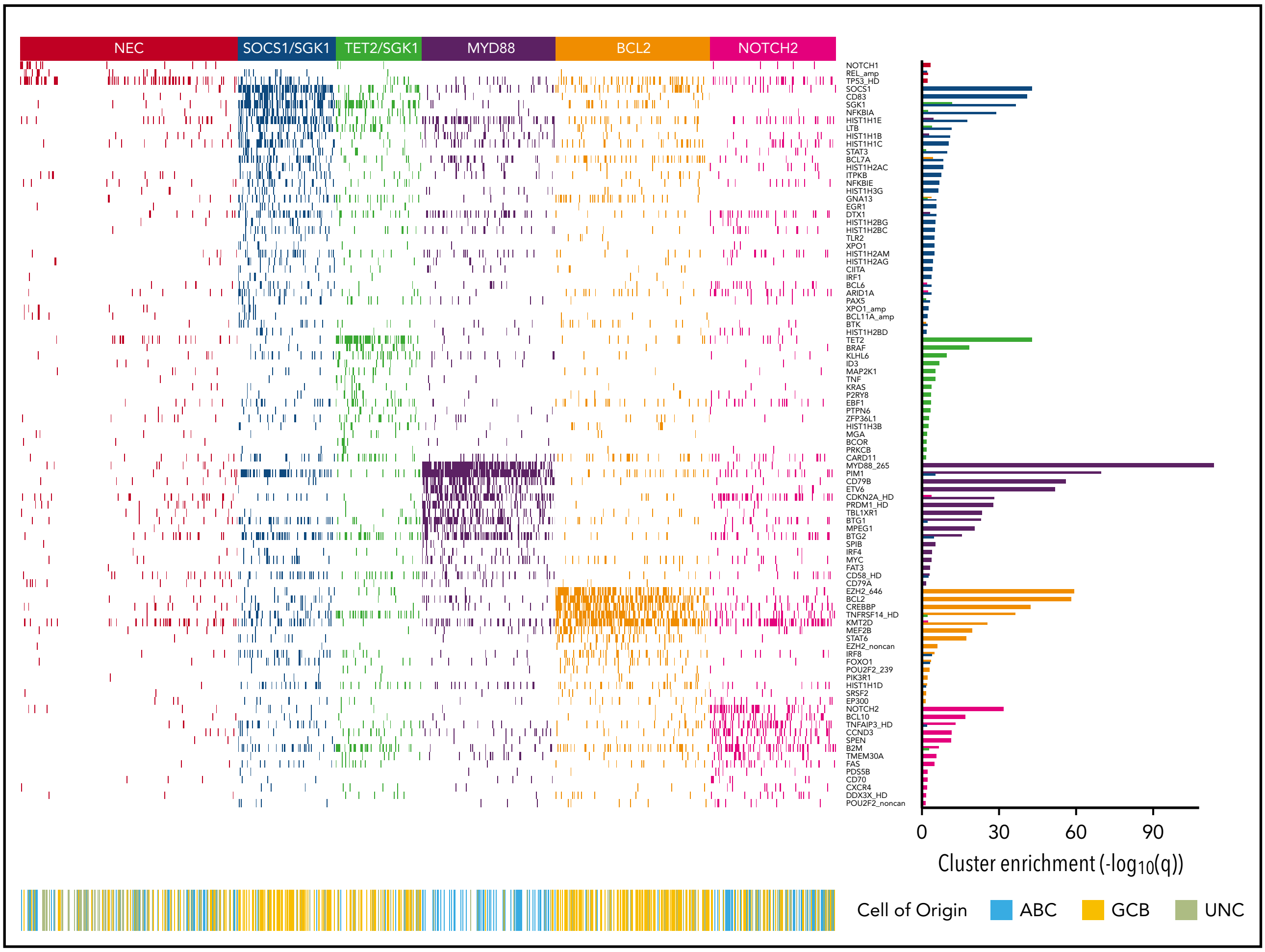

Figure 1. Heat map of characteristic mutations from each of the 6 genetic clusters that were identified by using the Akaike information criterion in the analysis cohort (n = 928). Distinct clusters are identified by color. Along the bottom of the figure, the color strip shows the corresponding cell-of-origin classification for each patient. The panel on the right-hand side shows the enrichment for mutations within each cluster, with a logarithmic *q*-value scale. Only those mutations are shown that are identified as significantly enriched for the given group, as determined by a Benjamini-Hochberg adjusted $q < 0.05$ from a χ^2 test of independence. "HD" indicates the homozygous deletion or a mutation in this gene; "noncan" denotes a non-canonical mutation; and "amp" indicates an amplification. For cell-of-origin, UNC represents the unclassified group.

well as those enriched in clusters within our patient cohort (supplemental Table 7). However, we were not able to resolve a division of the SGK1 subgroup, which in our cohort splits into SOCS1/SGK1 and TET2/SGK1 subgroups, a finding likely to be explained by the lack of *SOCS1* and *TET2* mutation calls in the data of Chapuy et al. Restricting the analysis to the 60 overlapping genetic features reproduced 5 of the original subgroups but led to loss of the cluster defined by TP53 mutation and copy number alteration (CNA), which corresponded to the C2 cluster of Chapuy et al (supplemental Figure 11). These cases were instead predominantly reassigned to the unclassified group (56%) and the BCL2 group (22.7%). Taken together, these findings confirm that our clustering approach is robust across data sets and that the absence of a TP53 cluster in our own cohort relates to limited copy number information available from our panel; the majority of cases likely to remain unclassified or allocated to the BCL2 group.

The clusters found in our main analysis are compared in summary vs those of Chapuy et al[17] and Schmitz et al[16] in Table 3. A detailed comparison with Chapuy et al is presented in the supplemental Methods (section 2.5).

Genomic subtype and patient outcome

Five-year overall survival (OS) estimates for all patients (n = 928) and those treated with R-CHOP (n = 648) are presented at the bottom of Table 2. For all patients, analyses revealed especially poor outcome for patients in the MYD88 cluster, with 5-year OS of 42% (34.9-50.7). In contrast, patients within the SOCS1/SGK1, BCL2, and TET2/SGK1 clusters fared better than patients in the MYD88 group, with 5-year OS of 64.9% (56.6-74.4), 62.5% (55.7-70.1), and 60.1% (51.1-70.6), respectively ($P < 10^{-3}$ for each group compared with MYD88). NEC and NOTCH2 clusters had intermediate survival: 5-year OS of 53.6% (47.7-60.2) and 48.1% (40.5-57.0) (P = .008, .063 compared with MYD88).

To examine survival in a more homogeneous patient cohort, we restricted our analysis to patients with de novo DLBCL NOS treated with curative intent (n = 690). Similar survival trends were observed, with the poorest outcome seen among the MYD88 subgroup (Figure 3A-B; supplemental Figure 12). Because some of these patients were treated with attenuated regimens that might be considered "R-CHOP–like," we repeated the analysis on the 579 patients with de novo DLBCL treated with R-CHOP (Figure 3C-D, supplemental Figure 12). Especially good survival

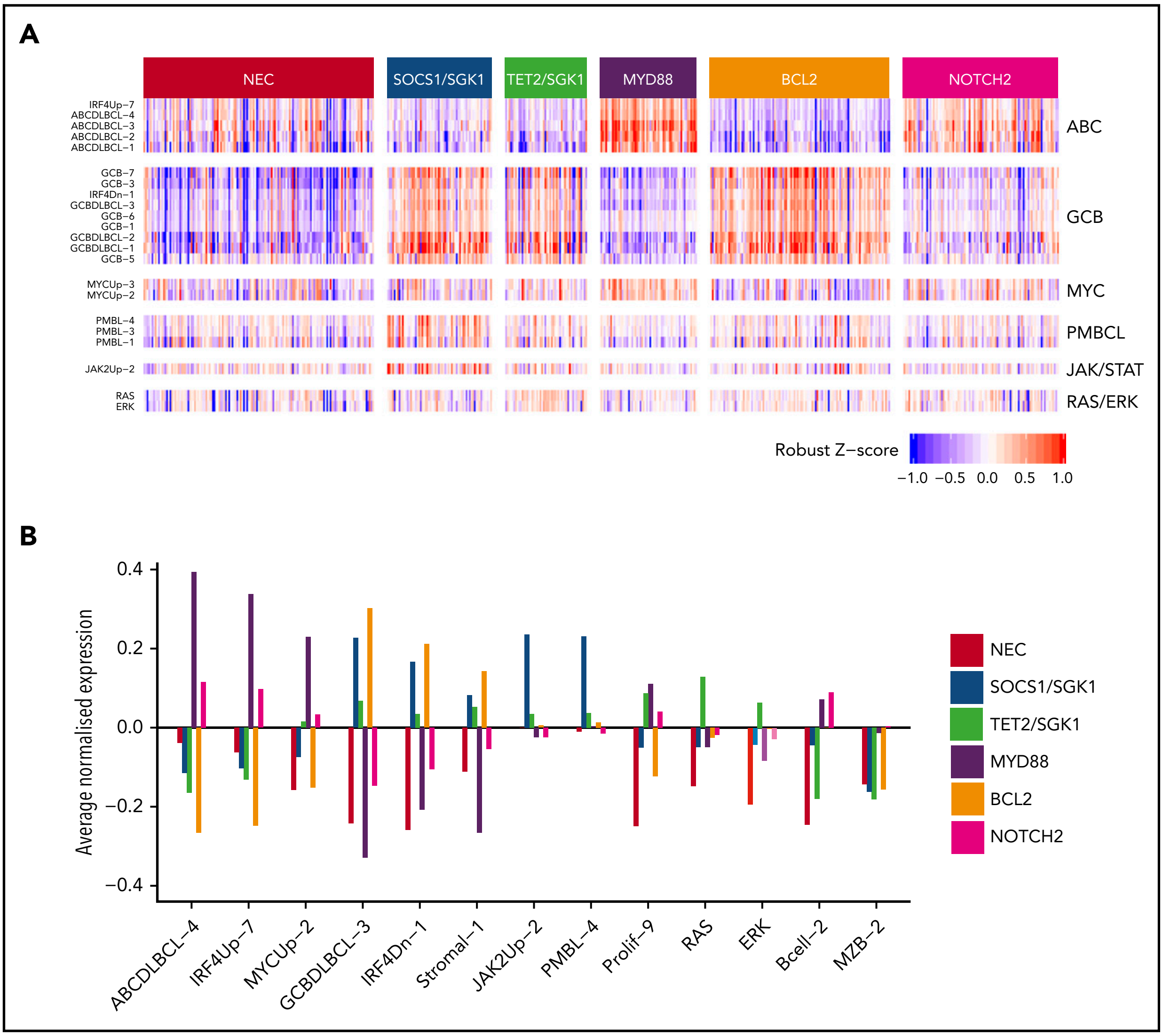

Figure 2. Relations between gene expression profiling and the 6 genetic clusters that were identified by using the Akaike information criterion for the 519 subjects with available gene expression profiling data. (A) Heat map of a selection of signatures. (B) Highlights of a small number of these that exhibit the strongest trends.

was seen in SOCS1/SGK1 (n = 84), in which 5-year OS was 80.2% (71.5-90.1). However, the apparently negative prognostic impact of MYD88 cluster membership (n = 78) was reduced, increasing the OS estimate of this subgroup to 62.8% (53.0-74.5); although not statistically significant (*P* = .1), this intriguing result suggests a specific sensitivity of the MYD88 subtype to either patient-intrinsic or treatment-related factors that may partially explain previous controversy regarding its prognostic implication.[31]

Inspection of clinical risk factors revealed variation across the molecular cluster; the NOTCH2 group was associated with the greatest number of patients with high-intermediate and high International Prognostic Index (IPI) scores (supplemental Figure 13). Figure 3 presents the IPI-adjusted hazard ratios for each molecular subtype, confirming inferior survival estimates in the MYD88 subtype, a neutral effect of NOTCH2, and enhanced survival in the TET2/SGK1, SOCS1/SGK1, and BCL2 groups.

Although our clustering algorithm did not resolve a distinct *NOTCH1* cluster, the majority of *NOTCH1* mutant cases were found within the unclassified NEC group, suggesting they may represent a distinct subtype too small to be detected by our modeling strategy. Indeed, the presence of *NOTCH1* mutation (n = 16) conferred an especially poor outcome, with a 5-year OS of 39% (NOTCH1 mutant vs wild type, *P* = .004) (Figure 4A).

MYC rearrangement was most enriched within the BCL2 cluster (supplemental Figure 13), conferring poor prognosis in R-CHOP–treated patients, 5-year OS 50.0% (31.5-79.4), compared vs patients without MYC rearrangement, who had 71% OS (62.4-81.8) (Figure 4B). Similarly, most cases of double-hit lymphoma and MHG were found in the BCL2 cluster, where both conferred a poor prognosis in R-CHOP–treated patients: 5-year OS 43.8% (25.1, 76.3) and 44.4% (21.4, 92.3), respectively. There were insufficient numbers of events to determine the effect of MYC rearrangement, double hit lymphoma, or MHG in other clusters (supplemental Figure 13). Also strongly enriched within the BCL2 cluster were cases of transformed follicular lymphoma and cases of DLBCL with a concurrent diagnosis of follicular lymphoma detected based on results of the diagnostic

Table 2. Characteristics according to AIC cluster: DLBCL diagnosed within HMRN, September 2004 to August 2012

Characteristic	Genetic subtype, n (%)					
	NEC	SOCS1/SGK1	TET2/SGK1	MYD88	BCL2	NOTCH2
All subtypes combined	248 (100)	111 (100)	98 (100)	152 (100)	176 (100)	143 (100)
DLBCL NOS	211 (85.1)	98 (88.3)	91 (92.9)	130 (85.5)	173 (98.3)	136 (95.1)
PCNSL	9 (3.6)	0 (0.0)	1 (1.0)	22 (14.5)	0 (0.0)	1 (0.7)
Primary mediastinal	2 (0.8)	12 (10.8)	0 (0.0)	0 (0.0)	3 (1.7)	3 (2.1)
T-cell/histiocyte-rich	16 (6.5)	1 (0.9)	2 (2.0)	0 (0.0)	0 (0.0)	2 (1.4)
Plasmablastic	9 (3.6)	0 (0.0)	4 (4.1)	0 (0.0)	0 (0.0)	1 (0.7)
Intravascular	1 (0.4)	0 (0.0)	0 (0.0)	0 (0.0)	0 (0.0)	0 (0.0)
De novo/transformed						
De novo	237 (95.6)	110 (99.1)	93 (94.9)	150 (98.7)	155 (88.1)	135 (94.4)
Transformed*	11 (4.4)	1 (0.9)	5 (5.1)	2 (1.3)	21 (11.9)	8 (5.6)
DLBCL with concurrent FL†	9 (3.6)	10 (9.0)	2 (2.0)	2 (1.3)	47 (26.7)	15 (10.5)
Testicular involvement‡	4 (2.8)	1 (1.8)	0 (0.0)	21 (26.9)	0 (0.0)	2 (3.1)
Breast involvement‡	2 (2.5)	0 (0.0)	1 (2.0)	9 (12.9)	1 (1.1)	0 (0.0)
Cell of origin§						
Classic						
GCB	43 (30.3)	56 (86.2)	33 (66.0)	5 (8.2)	92 (82.1)	36 (37.9)
ABC	38 (26.8)	4 (6.2)	5 (10.0)	50 (82.0)	3 (2.7)	42 (44.2)
Unclassified	61 (43.0)	5 (7.7)	12 (24.0)	6 (9.8)	17 (15.2)	17 (17.9)
Refined						
GCB	36 (25.4)	51 (78.5)	31 (62.0)	5 (8.2)	78 (69.6)	33 (34.7)
ABC	38 (26.8)	4 (6.2)	5 (10.0)	49 (80.3)	3 (2.7)	41 (43.2)
MHG	7 (4.9)	5 (7.7)	2 (4.0)	1 (1.6)	15 (13.4)	4 (4.2)
Unclassified	61 (43.0)	5 (7.7)	12 (24.0)	6 (9.8)	16 (14.3)	17 (17.9)
Age at diagnosis (range), y	67.0 (12.1-95.2)	66.8 (13.5-97.8)	72.7 (22.8-92.0)	70.2 (35.1-97.4)	66.4 (24.1-88.8)	70.2 (8.5-95.8)
R-CHOP treated	172 (69.4)	85 (76.6)	70 (71.4)	80 (52.6)	141 (80.1)	100 (69.9)
5-y OS (%, 95% CI)	53.6 (47.7-60.2)	64.9 (56.6-74.4)	60.1 (51.1-70.6)	42.1 (34.9-50.7)	62.5 (55.7-70.1)	48.1 (40.5-57.0)
R-CHOP treated (%, 95% CI)	65.6 (58.9-73.1)	80.0 (71.9-89.0)	69.8 (59.8-81.5)	63.8 (54.0-75.2)	69.5 (62.3-77.5)	58.8 (49.8-69.3)

Data are presented as n (%) unless otherwise indicated. AIC, Akaike information criterion; CI, confidence interval; FL, follicular lymphoma; OS, overall survival.

*Prior diagnosis: 22 FLs, 14 marginal zone lymphomas, 7 chronic lymphocytic leukemias, 2 hairy cell leukemias, and 3 Hodgkin lymphomas.

†Includes FL discovered at time of DLBCL diagnosis, excluding those with prior FL diagnosis.

‡Sex-specific proportions.

§Percentage of those with material available.

biopsy. Although patients with transformed follicular lymphoma had inferior survival estimates, in the BCL2 cluster, no differences in survival between DLBCL with/without a concurrent diagnosis of follicular lymphoma was observed. This finding agrees with a recent study by Wang et al[32] (supplemental Figure 14).

As noted earlier, we did not identify a distinct TP53/CNA cluster in our cohort. The potential for other clusters, in particular the BCL2 subgroup, to contain cases that might otherwise have been classified to a TP53 cluster prompted us to examine survival of each cluster stratified according to TP53 mutation status. Remarkably, the prognostic impact of TP53 mutation (Figure 4C) varied considerably across the different molecular subtypes (Figure 4D). *TP53* mutation was associated with a worse prognosis in the NEC and BCL2 subtypes and, although uncommon, *TP53* mutation conferred an extremely poor prognosis in the MYD88 cluster. In contrast, there was no evidence of a prognostic effect in patients within the NOTCH2 or SOCS1/SGK1 clusters, and was rarely detected in the TET2/SGK1 cluster. This finding suggests that in addition to its presence in a TP53-mutant cluster, TP53 mutation may also be acquired by tumors belonging to other subgroups and that in this scenario its prognostic effect is subtype dependent.

Discussion

Based on the genomic profile of individual tumors, our large population-based study defined 5 molecular DLBCL subtypes, named MYD88, BCL2, SOCS1/SGK1, TET2/SGK1, and NOTCH2, with each having distinct features in terms of both their biology and clinical outcome. With prospective tracking of treatment and outcome in 928 patients with DLBCL (trial and nontrial) diagnosed by specialist staff at a single laboratory, we escape the biases that may result from sequencing archived biopsy collections

Table 3. Comparison of main clusters

Current study	Chapuy et al[17]	Schmitz et al[16]	Notes
MYD88 MYD88, PIM1, CD79B, ETV6, CDKN2A	**C5** CD79B, MYD88, ETV6, PIM1, TBL1XR1	**MCD** MYD88, CD79B	Strongly associated with ABC-type DLBCL. The most robust group, occurring in all reports. Contains the majority of cases with PCNSL and primary testicular lymphoma. Associated with a poor prognosis
BCL2 EZH2, BCL2, CREBBP, TNFRSF14, KMT2D	**C3** BCL2, CREBBP2, EZH2, KMT2D, TNFRSF14	**EZB** BCL2 translocation, EZH2	Strongly associated with GCB-type DLBCL. Mutational profile is shared with follicular lymphoma. Contains the majority of cases of transformed follicular lymphoma and cases with a concurrent diagnosis of follicular lymphoma. Generally favorable prognosis, although enriched for cases of double-hit lymphoma and MHG
SOCS1/SGK1 SOCS1, CD83, SGK1, NFKBIA, HIST1H1E	**C4** SGK1, HIST1H1E, NFKBIE, BRAF, CD83		Predominantly GCB-type DLBCL. Shares genetic and gene expression features of PMBCL. Associated with the most favorable prognosis
TET2/SGK1 TET2, BRAF, SGK1, KLHL6, ID3			A less strongly identifiable subtype emerging from SGK1 when applying the Akaike information criterion (supplemental Methods). Has very strong similarity to SOCS1/SGK1 but differentiated by the addition of TET2 and BRAF and the lack of SOCS1 and CD83. Associated with a favorable prognosis
NOTCH2 NOTCH2, BCL10, TNFAIP3, CCND3, SPEN	**C1** BCL6 translocation, BCL10, TNFAIP3, UBE2A, CD70	**BN2** BCL6 translocation, NOTCH2	Not associated with any cell of origin. Shares mutational similarity to MZL but not enriched for cases of transformed MZL. Less strongly defined than other subgroups (supplemental Methods)
NEC NOTCH1, REL amplification, TP53		**Other**	A default category, containing cases that could not be classified elsewhere. Contains cases with no detected mutation. Likely to also contain cases belonging to both NOTCH1 and TP53/CNA subgroups. Even though 3 abnormalities are significantly enriched in this group, their q-values are far less extreme than those of characteristic mutations from the other subtypes
	C2 TP53, frequent deletions		Characterized by TP53 mutation and widespread copy number changes. Due to limited CNA in our study, these cases were predominantly allocated to the NEC group
	C0 No detected abnormalities		Cases with no detectable mutation were allocated to the NEC group
		N1 **NOTCH1**	Characterized by NOTCH1 mutation, this was significantly elevated in our NEC group but only mutated in 2.5% of samples. Associated with poor outcome

MZL, marginal zone lymphoma.

established from the selective referral of clinically or diagnostically challenging cases to specialist pathology centers. Indeed, the only determinant of whether patients were included in the analysis cohort was the availability of sufficient sample for the extraction of adequate DNA. This unselected cohort therefore provides a unique representation of real-world DLBCL that may not have been captured in previous molecular subtyping studies. We have not restricted the cluster analysis to any particular subtype of DLBCL, considering an a priori approach to the evolving classification of these possibly heterogeneous disease types a particular strength of this study.

Considerable variability in genomic subtype identification can be introduced by differences in biopsy type, sequencing strategy, variant calling pipeline, driver annotation algorithms, and the statistical method used to identify genomic clusters. It remained uncertain whether the genomic clusters described in recent studies represented sufficiently robust entities to be resolved against variation in each of the aforementioned factors. We used alternative, but widely accepted, pipelines for variant and driver annotation and different approaches to the identification of genomic clusters. Despite these considerable differences, we have independently converged on very similar genomic subtypes. Indeed, when comparing enriched mutations between equivalent clusters across studies, we observe a very high degree of overlap. Therefore, our data strongly support the conclusion that DLBCL exists as molecularly distinct subtypes that are resolvable through genomic analysis. Importantly, we were able to identify these subtypes by using a targeted sequencing panel applied to biopsy material, a strategy that would be applicable to a nonacademic diagnostic laboratory.

The lack of BCL6 fusion data is a limitation of our study. However, available FISH data confirmed the association between *NOTCH2* mutation and rearrangement of *BCL6*. Furthermore, even in the absence of *BCL6* fusion data, we were able to identify a *NOTCH2* subtype that shows mutation enrichment similar to the previously identified BN2/C1[16,17] clusters. Our study was also limited by the extent of copy number data available from our panel. As such, we did not resolve a subgroup mapping to the C2 cluster of Chapuy et al.[17] The application of our clustering algorithm to the data of Chapuy et al, applying all or just overlapping genetic features, supports the existence of this subtype and the requirement for adequate copy number information for its detection. Future sequencing panels designed to assign DLBCL molecular subtype will likely include probes that target regions of recurrent copy number variability. The existence of a TP53/CNA cluster is further supported by the finding that the majority (56%) of these cases were not alternatively classified but rather assigned to an unclassified NEC group according to our cluster algorithm (supplemental Figure 11). However, 23% of the TP53/CNA cases carried a mutational profile that, in the absence of copy number data, reassigns them to the BCL2 cluster. This leads us to hypothesize that TP53 mutation and associated CNAs may arise in 2 different contexts: either as the primary determinant of a distinct disease subtype or alternatively as a secondary event in a tumor arising from one of the other subgroups, most commonly the BCL2 cluster.

A novel finding in our study was the division of the previously identified SGK1 cluster[17] into SOCS1/SGK1 and TET2/SGK1 subgroups, the biological validity of which was supported by the enrichment of JAK/STAT and ERK gene expression signatures, respectively. Driver mutations of *TET2* and *SOCS1* were not reported in the earlier study,[17] which impaired the ability of our clustering algorithm to resolve this split within the data of Chapuy et al. These differences in mutation calling, likely due to differences in variant and driver annotation strategies, highlight some of the challenges to be overcome when implementing a consensus classification system. Interestingly, our SOCS1/SGK1 subtype shared both mutation and gene expression profile similarities with PMBCL, supporting a previous description of non-mediastinal DLBCL tumors that share biological similarity with PMBCL.[29] This analysis also has parallels with other subsets of special site lymphomas, including PCNSL and those occurring de novo in testis and breast, which overlap with the MYD88 subgroup; this finding highlights a recurrent link between special site and nodal DLBCL NOS across several molecular subsets.

Prospective clinical data on all cases (supplemental Table 4) provided greater insight into the prognostic impact of clusters, revealing how survival of MYD88 clustered patients was especially sensitive to either patient-intrinsic or treatment-related characteristics. This difference in outcome when analysis of MYD88 patients is restricted to those treated with full R-CHOP vs other R-CHOP–like regimens may explain some of the controversy around the prognostic impact of this group.[31] Multivariate analysis allowed us to quantify the relative risk of individual subtypes independent of IPI factors, an analysis that reinforced the importance of clinical risk factors in determining prognosis. Most notably, we have revealed the extremely favorable outcome of patients in the SOCS1/SGK1 subtype, suggesting this group might be the subject of future trials examining de-escalation of therapy.

The large size of our cohort allowed us to examine the impact of individual factors within clusters. Of particular interest, we were able to comment on the survival of patients in the BCL2 cluster with and without concurrent follicular lymphoma according to results of the diagnostic biopsy. The similarity of survival in response to R-CHOP mirrors that recently reported[32] and leads us to hypothesize that DLBCL with concurrent follicular lymphoma may represent an entity that is biologically and clinically indistinguishable from other DLBCL patients clustered into the BCL2 subgroup, with the finding of concurrent follicular lymphoma dependent solely on the region of tumor captured by the biopsy finding. Conversely, transformed follicular lymphoma was associated with inferior survival, consistent with this form representing a distinct clinical entity.

Individual genetic features allowed us to identify other high-risk groups. Although we did not identify a distinct *NOTCH1* cluster, the predominance of *NOTCH1* mutant cases within the NEC group and their especially poor outcome support the concept that these patients should be considered separately in clinical practice. Many (27 of 66) translocated lymphomas, and the majority (21 of 38) of double-hit lymphomas, were classified into the BCL2 cluster, allowing very good and poor risk subgroups to be resolved from this cluster. Finally, we observe intriguing variation of the impact of TP53 mutation across clusters with no detectable effect in the NOTCH2 group, contrasting with the dismal prognosis conferred in the MYD88 cluster. Overall, this suggests that individual prognostic information may ultimately

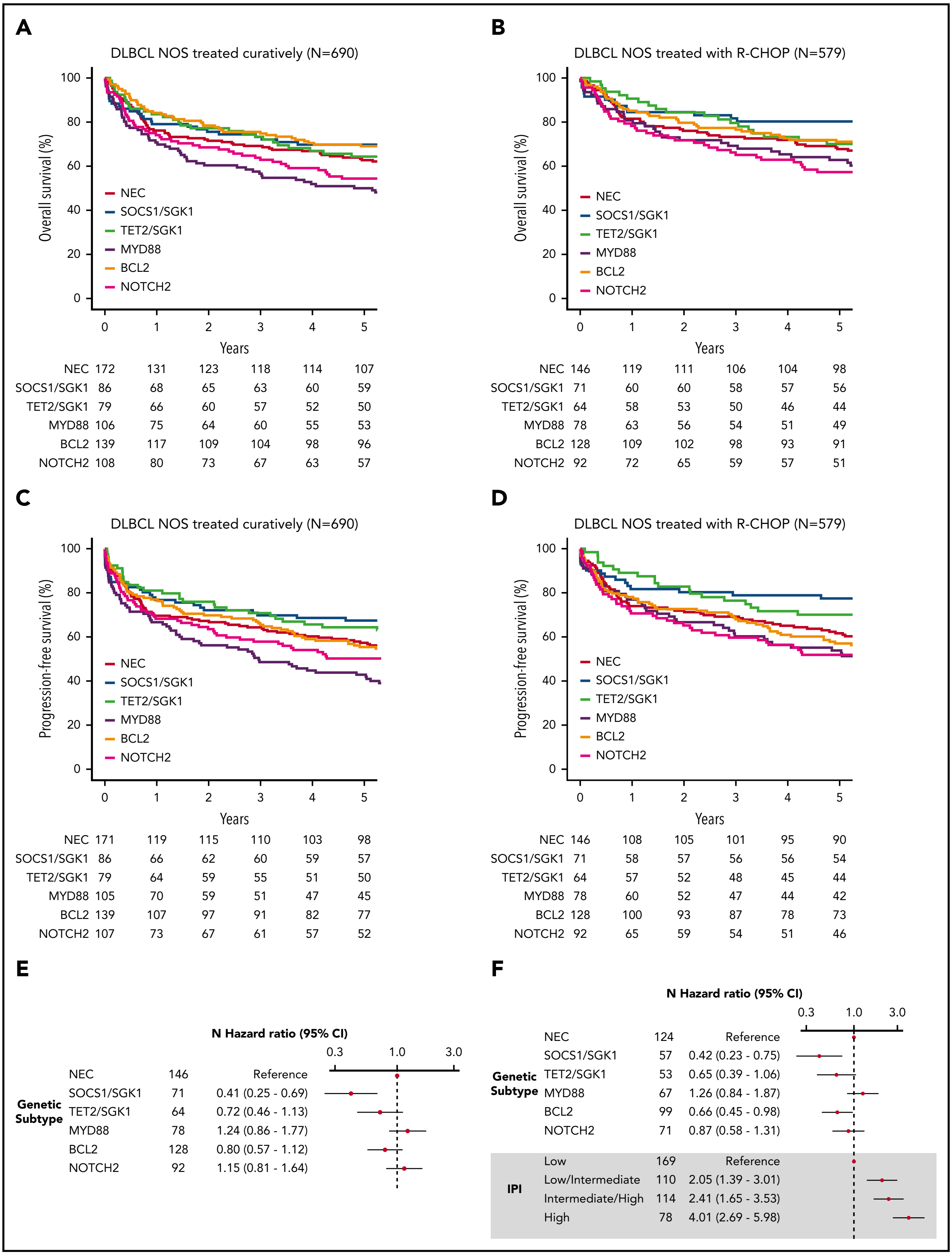

A

	0	1	2	3	4	5
NEC	172	131	123	118	114	107
SOCS1/SGK1	86	68	65	63	60	59
TET2/SGK1	79	66	60	57	52	50
MYD88	106	75	64	60	55	53
BCL2	139	117	109	104	98	96
NOTCH2	108	80	73	67	63	57

B

	0	1	2	3	4	5
NEC	146	119	111	106	104	98
SOCS1/SGK1	71	60	60	58	57	56
TET2/SGK1	64	58	53	50	46	44
MYD88	78	63	56	54	51	49
BCL2	128	109	102	98	93	91
NOTCH2	92	72	65	59	57	51

C

	0	1	2	3	4	5
NEC	171	119	115	110	103	98
SOCS1/SGK1	86	66	62	60	59	57
TET2/SGK1	79	64	59	55	51	50
MYD88	105	70	59	51	47	45
BCL2	139	107	97	91	82	77
NOTCH2	107	73	67	61	57	52

D

	0	1	2	3	4	5
NEC	146	108	105	101	95	90
SOCS1/SGK1	71	58	57	56	56	54
TET2/SGK1	64	57	52	48	45	44
MYD88	78	60	52	47	44	42
BCL2	128	100	93	87	78	73
NOTCH2	92	65	59	54	51	46

E

		N	Hazard ratio (95% CI)
Genetic Subtype	NEC	146	Reference
	SOCS1/SGK1	71	0.41 (0.25 - 0.69)
	TET2/SGK1	64	0.72 (0.46 - 1.13)
	MYD88	78	1.24 (0.86 - 1.77)
	BCL2	128	0.80 (0.57 - 1.12)
	NOTCH2	92	1.15 (0.81 - 1.64)

F

		N	Hazard ratio (95% CI)
Genetic Subtype	NEC	124	Reference
	SOCS1/SGK1	57	0.42 (0.23 - 0.75)
	TET2/SGK1	53	0.65 (0.39 - 1.06)
	MYD88	67	1.26 (0.84 - 1.87)
	BCL2	99	0.66 (0.45 - 0.98)
	NOTCH2	71	0.87 (0.58 - 1.31)
IPI	Low	169	Reference
	Low/Intermediate	110	2.05 (1.39 - 3.01)
	Intermediate/High	114	2.41 (1.65 - 3.53)
	High	78	4.01 (2.69 - 5.98)

Figure 3. Survival in clusters identified by using the Akaike information criterion. (A) OS of the 690 patients treated with curative intent stratified according to cluster. (B) OS of the 579 de novo DLBCL NOS patients treated using R-CHOP, stratified according to cluster. (C) Progression-free survival of the 690 patients treated with curative intent stratified according to cluster. (D) Progression-free survival of the 579 de novo DLBCL NOS patients treated by using R-CHOP, stratified according to cluster. (E) Crude hazard ratios of cluster membership for the 579 de novo DLBCL NOS R-CHOP–treated patients. (F) Adjusted hazard ratios of the subset of the group of 579 patients with IPI data available (n = 499). CI, confidence interval.

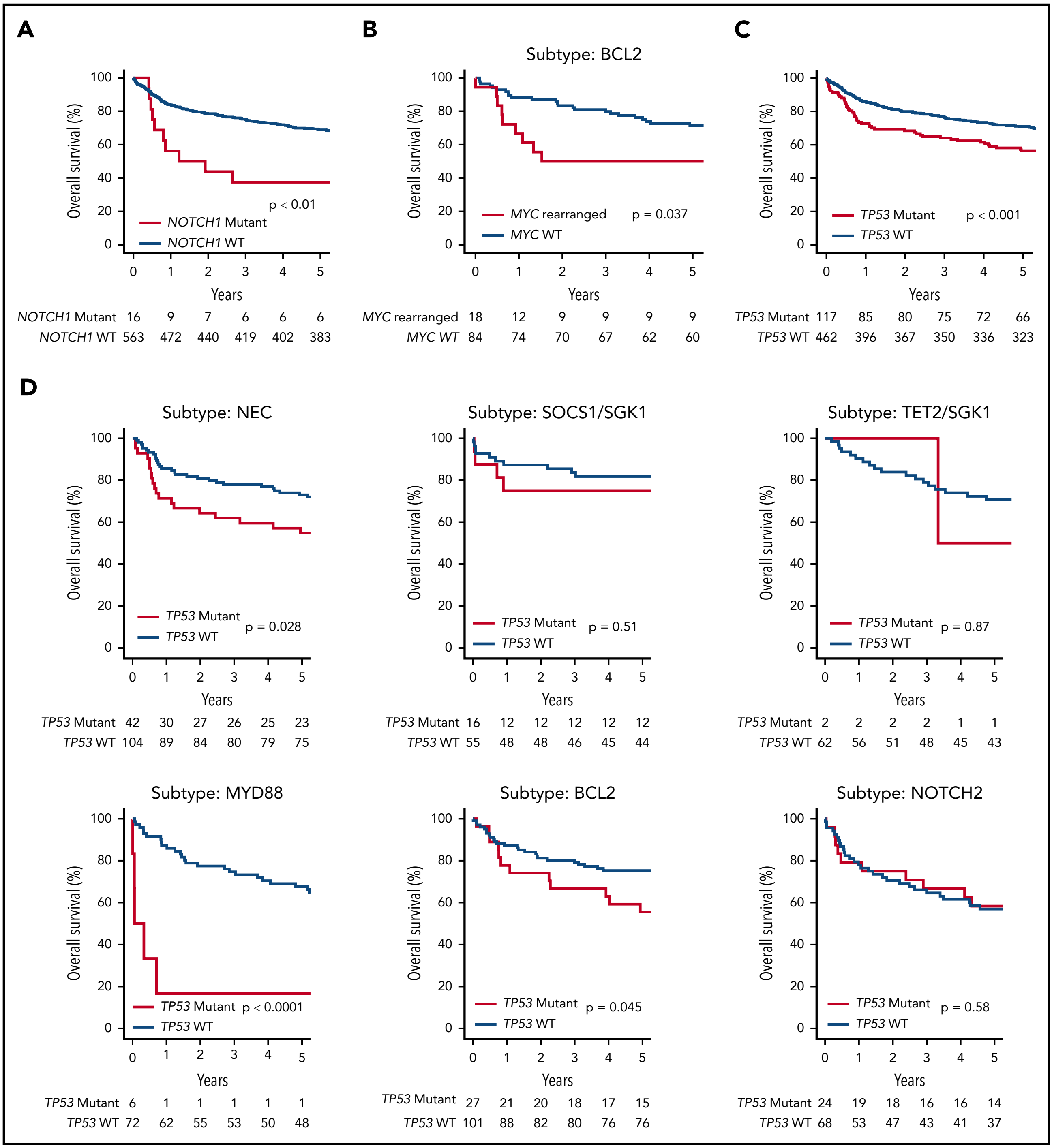

Figure 4. OS of the de novo DLBCL NOS R-CHOP–treated patients (n = 579), stratified according to a selection of genetic features. (A) NOTCH1 mutation. (B) MYC rearrangement status in the subset of patients belonging to the BCL2 Akaike information criterion subtype. (C) TP53 mutation or homozygous deletion. (D) The effect of TP53 mutation or homozygous deletion in each genetic subtype.

be best tailored to patients through the combined use of genomic cluster and individual gene data.

This study is the first to analyze the genetic structure of DLBCL by using a large unselected population-based register of patients with full clinical follow-up. Our findings substantiate the conclusions of recent studies by confirming the existence of reproducible molecular subtypes of DLBCL defined by their profile of genomic alterations. We show that genetic subtypes can be resolved by using a targeted sequencing panel applied to biopsy material acquired in routine clinical practice. We refined the molecular classification further to identify a new, very good risk subtype that shares biological features of PMBCL. We also provide greater insight into the prognostic impact of the genomic subtypes and their interaction with other genetic and clinical factors. Together with previous studies, these findings suggest that the field is ready for a concerted effort to standardize the molecular subclassification of DLBCL. Stratification according to molecular subtype will guide the design and interpretation of future clinical trials in DLBCL.

Acknowledgments

Bloodwise (grant 15037) funded the majority of this study. Genetic sequencing was funded by 14M Genomics, a start-up company that ceased trading February 2016. Bloodwise had no role in the design of the study, data collection, data analysis, data interpretation, or writing of the report. 14M Genomics was involved in the design of the pan-hematological gene panel but took no further part in the study. D.J.H. was funded by a clinician scientist fellowship from the Medical Research Council (MRC) and receives core funding from Wellcome and MRC to the Wellcome–MRC Cambridge Stem Cell Institute. Some of the analysis in this study was performed on the "Viking" high-performance computing cluster at the University of York.

Authorship

Contribution: S.L.B., P.A.B., D.P., A.G.S., E.R., P.J.C., R.M.T., R.P., C.B., and S.C. contributed to conception and design; S.L.B., P.A.B., D.P., A.G.S., E.R., S.L.C., P.G., S.J.L.V.H., N.W., P.J.C., R.P., C.B., and S.C. provided study material or patients; all authors participated in the collection and assembly of data; S.E.L., S.L.B., P.A.B., D.P., A.G.S., E.R., S.L.C., C.R., P.J.C., R.M.T., R.P., C.B., S.C., and D.J.H. analyzed and interpreted the data; S.E.L., S.L.B., P.A.B., A.G.S., E.R., C.B., S.C., and D.J.H. wrote the manuscript; and all authors gave final approval of the manuscript and agreed to be accountable for all aspects of the work.

Conflict-of-interest disclosure: P.A.B. reports consultancy for Karus Therapeutics, OncoDNA, and Everything Genetic. D.J.H. received research funding from Gilead International; and reports consultancy for Karus. The remaining authors declare no competing financial interests.

The current affiliation for C.R. is Department of Bioengineering, Stanford University, Palo Alto, CA.

ORCID profiles: D.P., 0000-0002-3936-7569; A.G.S., 0000-0002-1111-966X; E.R., 0000-0001-7603-3704; C.R., 0000-0002-8395-2853; S.C., 0000-0002-3026-2859; D.J.H., 0000-0001-6225-2033.

Correspondence: Simon Crouch, Epidemiology and Cancer Statistics Group, Department of Health Sciences, University of York, York, YO10 5DD, United Kingdom; e-mail: simon.crouch@york.ac.uk.

Footnotes

Submitted 27 September 2019; accepted 9 February 2020; prepublished online on *Blood* First Edition 18 March 2020. DOI 10.1182/blood.2019003535.

*S.E.L., S.L.B., and P.A.B. are joint first authors.

†C.B., S.C., and D.J.H. are joint senior authors.

The online version of this article contains a data supplement.

There is a *Blood* Commentary on this article in this issue.

The publication costs of this article were defrayed in part by page charge payment. Therefore, and solely to indicate this fact, this article is hereby marked "advertisement" in accordance with 18 USC section 1734.

REFERENCES

1. Smith A, Crouch S, Lax S, et al. Lymphoma incidence, survival and prevalence 2004-2014: sub-type analyses from the UK's Haematological Malignancy Research Network. *Br J Cancer.* 2015;112(9):1575-1584.

2. Swerdlow S, Campo E, Harris N, et al. WHO Classification of Tumours of Haematopoietic and Lymphoid Tissues. Lyon, France: World Health Organization; 2017.

3. Teras LR, DeSantis CE, Cerhan JR, Morton LM, Jemal A, Flowers CR. 2016 US lymphoid malignancy statistics by World Health Organization subtypes. *CA Cancer J Clin.* 2016; 66(6):443-459.

4. Coiffier B, Lepage E, Briere J, et al. CHOP chemotherapy plus rituximab compared with CHOP alone in elderly patients with diffuse large-B-cell lymphoma. *N Engl J Med.* 2002; 346(4):235-242.

5. Alizadeh AA, Eisen MB, Davis RE, et al. Distinct types of diffuse large B-cell lymphoma identified by gene expression profiling. *Nature.* 2000;403(6769):503-511.

6. Wright G, Tan B, Rosenwald A, Hurt EH, Wiestner A, Staudt LM. A gene expression-based method to diagnose clinically distinct subgroups of diffuse large B cell lymphoma. *Proc Natl Acad Sci U S A.* 2003;100(17): 9991-9996.

7. Sha C, Barrans S, Cucco F, et al. Molecular high-grade B-cell lymphoma: defining a poor-risk group that requires different approaches to therapy. *J Clin Oncol.* 2019;37(3):202-212.

8. Painter D, Barrans S, Lacy S, et al. Cell-of-origin in diffuse large B-cell lymphoma: findings from the UK's population-based Haematological Malignancy Research Network. *Br J Haematol.* 2019;185(4):781-784.

9. Pasqualucci L, Trifonov V, Fabbri G, et al. Analysis of the coding genome of diffuse large B-cell lymphoma. *Nat Genet.* 2011;43(9): 830-837.

10. Morin RD, Mendez-Lago M, Mungall AJ, et al. Frequent mutation of histone-modifying genes in non-Hodgkin lymphoma. *Nature.* 2011;476(7360):298-303.

11. Lohr JG, Stojanov P, Lawrence MS, et al. Discovery and prioritization of somatic mutations in diffuse large B-cell lymphoma (DLBCL) by whole-exome sequencing. *Proc Natl Acad Sci U S A.* 2012;109(10): 3879-3884.

12. Monti S, Chapuy B, Takeyama K, et al. Integrative analysis reveals an outcome-associated and targetable pattern of p53 and cell cycle deregulation in diffuse large B cell lymphoma. *Cancer Cell.* 2012;22(3): 359-372.

13. Morin RD, Mungall K, Pleasance E, et al. Mutational and structural analysis of diffuse large B-cell lymphoma using whole-genome sequencing. *Blood.* 2013;122(7):1256-1265.

14. de Miranda NFCC, Georgiou K, Chen L, et al. Exome sequencing reveals novel mutation targets in diffuse large B-cell lymphomas derived from Chinese patients. *Blood.* 2014; 124(16):2544-2553.

15. Karube K, Enjuanes A, Dlouhy I, et al. Integrating genomic alterations in diffuse large B-cell lymphoma identifies new relevant pathways and potential therapeutic targets. *Leukemia.* 2018;32(3):675-684.

16. Schmitz R, Wright GW, Huang DW, et al. Genetics and pathogenesis of diffuse large B-cell lymphoma. *N Engl J Med.* 2018; 378(15):1396-1407.

17. Chapuy B, Stewart C, Dunford AJ, et al. Molecular subtypes of diffuse large B cell lymphoma are associated with distinct pathogenic mechanisms and outcomes [published corrections appear in Nat Med. 2018;24(8):1292, Nat Med. 2018;24(8): 1290-1291]. *Nat Med.* 2018;24(5): 679-690.

18. Reddy A, Zhang J, Davis NS, et al. Genetic and functional drivers of diffuse large B cell lymphoma. *Cell.* 2017;171(2):481-494.e15.

19. Smith A, Howell D, Crouch S, et al. Cohort profile: the Haematological Malignancy Research Network (HMRN): a UK population-based patient cohort. *Int J Epidemiol.* 2018; 47(3):700-700g.

20. Smith A, Roman E, Howell D, Jones R, Patmore R, Jack A; Haematological Malignancy Research Network. The Haematological Malignancy Research Network (HMRN): a new information strategy for population based epidemiology and health service research. *Br J Haematol.* 2010;148(5):739-753.

21. Leisch F. FlexMix: a general framework for finite mixture models and latent class regression in R. *J Stat Softw.* 2004; 11(1):1-18.

22. Biernacki C, Celeux G, Govaert G. Assessing a mixture model for clustering with the integrated completed likelihood. *IEEE Trans Pattern Anal Mach Intell.* 2000;22(7): 719-725.

23. Monti S, Tamayo P, Mesirov J, Golub T. consensus clustering: a resampling-based method for class discovery and visualization of gene expression microarray data. *Mach Learn*. 2003;52(1):91-118.

24. Stata Corp. Stata Statistical Software: Release 15. College Station, TX: Stata Corp; 2017.

25. R Core Team. R: A language and environment for statistical computing. Vienna, Austria: R Foundation for Statistical Computing; 2019.

26. Therneau TM, Grambsch PM. Modeling Survival Data: Extending the Cox Model. New York, NY: Springer-Verlag; 2000.

27. Mootha VK, Lindgren CM, Eriksson KF, et al. PGC-1α-responsive genes involved in oxidative phosphorylation are coordinately downregulated in human diabetes. *Nat Genet*. 2003;34(3):267-273.

28. Subramanian A, Tamayo P, Mootha VK, et al. Gene set enrichment analysis: a knowledge-based approach for interpreting genome-wide expression profiles. *Proc Natl Acad Sci U S A*. 2005;102(43):15545-15550.

29. Yuan J, Wright G, Rosenwald A, et al; Lymphoma Leukemia Molecular Profiling Project (LLMPP). Identification of primary mediastinal large B-cell lymphoma at nonmediastinal sites by gene expression profiling. *Am J Surg Pathol*. 2015;39(10): 1322-1330.

30. Mottok A, Hung SS, Chavez EA, et al. Integrative genomic analysis identifies key pathogenic mechanisms in primary mediastinal large B-cell lymphoma. *Blood*. 2019; 134(10):802-813.

31. Wright GW, Wilson WH, Staudt LM. Genetics of diffuse large B-cell lymphoma. *N Engl J Med*. 2018;379(5):493-494.

32. Wang Y, Link BK, Witzig TE, et al. Impact of concurrent indolent lymphoma on the clinical outcome of newly diagnosed diffuse large B-cell lymphoma. *Blood*. 2019;134(16): 1289-1297.